Title
Carbon-Carbon Bond Cleavage in Activation of the Prodrug Nabumetone

Journal
Drug Metabolism and Disposition, 42(5)

ISSN
0090-9556

Authors
Varfaj, Fatbardha
Zulkifli, Siti NA
Park, Hyoung-Goo
et al.

Publication Date
2014-05-01

DOI
10.1124/dmd.114.056903

Peer reviewed

1521-009X/42/5/828–838$25.00
Drug Metabolism and Disposition
http://dx.doi.org/10.1124/dmd.114.056903
Drug Metab Dispos 42:828–838, May 2014

Carbon-Carbon Bond Cleavage in Activation of the Prodrug Nabumetone[S]

Fatbardha Varfaj, Siti N. A. Zulkifli, Hyoung-Goo Park, Victoria L. Challinor, James J. De Voss, and Paul R. Ortiz de Montellano

Department of Pharmaceutical Chemistry, University of California, San Francisco, California (F.V., H.P., P.R.O.M.); Department of Chemistry, University of Queensland, St. Lucia, Brisbane, Australia (S.N.A.Z., V.L.C., J.J.D.V.); and Department of Biological Sciences, Konkuk University, Seoul, Korea (H.P.)

Received January 9, 2014; accepted February 28, 2014

ABSTRACT

Carbon-carbon bond cleavage reactions are catalyzed by, among others, lanosterol 14-demethylase (CYP51), cholesterol side-chain cleavage enzyme (CYP11), sterol 17β-lyase (CYP17), and aromatase (CYP19). Because of the high substrate specificities of these enzymes and the complex nature of their substrates, these reactions have been difficult to characterize. A CYP1A2-catalyzed carbon-carbon bond cleavage reaction is required for conversion of the prodrug nabumetone to its active form, 6-methoxy-2-naphthylacetic acid (6-MNA). Despite worldwide use of nabumetone as an anti-inflammatory agent, the mechanism of its carbon-carbon bond cleavage reaction remains obscure. With the help of authentic synthetic standards, we report here that the reaction involves 3-hydroxylation, carbon-carbon cleavage to the aldehyde, and oxidation of the aldehyde to the acid, all catalyzed by CYP1A2 or, less effectively, by other P450 enzymes. The data indicate that the carbon-carbon bond cleavage is mediated by the ferric peroxo anion rather than the ferryl species in the P450 catalytic cycle. CYP1A2 also catalyzes *O*-demethylation and alcohol to ketone transformations of nabumetone and its analogs.

Introduction

Nabumetone, one of the most commonly used nonsteroidal anti-inflammatory drugs because of its unique pharmacokinetic profile and special safety features in pharmacodynamic terms (Hedner et al., 2004), is used to reduce pain and inflammation in patients suffering from osteoarthritis or rheumatoid arthritis. Nabumetone is actually a prodrug that exerts its pharmacological effects via its metabolite 6-methoxy-2-naphthylacetic acid (6-MNA) (Hedner et al., 2004). Although 6-MNA may have additional physiologic effects, its anti-inflammatory properties are attributed to its ability to decrease prostaglandin synthesis by inhibiting cyclooxygenase 2.

After oral administration, nabumetone undergoes hepatic oxidative cleavage of the aliphatic side chain to yield 6-MNA, the physiologically active metabolite (Mangan et al., 1987). In addition, two minor metabolic pathways have been observed, one that involves *O*-demethylation and the other reduction of the ketone to the alcohol (Haddock et al., 1984). Approximately 35% of a 1-g oral dose of nabumetone is converted to 6-MNA, whereas 50% is converted into unidentified metabolites that are subsequently excreted in the urine [DrugBank, Accession number DB00461 (APRD01128), http://www.drugbank.ca/drugs/DB00461]. 6-MNA undergoes further metabolism by CYP2C9 to the inactive metabolite 6-hydroxy-2-naphthylacetic acid (Matsumoto et al., 2011).

The relative activities of individual cytochrome P450 enzymes in the conversion of nabumetone to 6-MNA and studies of microsomes with inhibitors indicated that CYP1A2, which had the highest activity, accounted for more than 50% of the conversion, with smaller contributions by CYP2B6, CYP2C19, CYP2D6, and CYP2E1 (Turpeinen et al., 2009). However, the detailed mechanism of the cytochrome P450-catalyzed conversion of nabumetone to 6-MNA remains unknown. In this study, we elucidate the metabolic steps leading to the formation of 6-MNA from nabumetone by CYP1A2 and other P450 enzymes.

Materials and Methods

All materials and reagents were of the highest commercial grade available. Glucose-6-phosphate, glucose-6-phosphate dehydrogenase, bovine liver catalase, β-nicotinamide adenine dinucleotide phosphate, magnesium chloride, α-naphthoflavone, phenacetin, cumene hydroperoxide, ampicillin, lysozyme, isopropyl β-D-thiogalactoside, phenylmethanesulfonyl fluoride, CH_2Cl_2-d_2, and monobasic and dibasic potassium phosphate were purchased from Sigma-Aldrich (St. Louis, MO). 7-Ethoxyresorufin and 7-hydroxyresorufin were obtained from Molecular Probes (Eugene, OR), nabumetone from Santa Cruz Biotechnology (Dallas, TX), [^{13}C,^{2}H$_3$]nabumetone from Alsachim (Strasbourg, France), and 6-MNA from Cayman Chemical Company (Ann Arbor, MI). EDTA- and Ca^{2+}-free protease inhibitor mixture was purchased from Roche (Basel, Switzerland). The high-performance liquid chromatography (HPLC) grade solvents acetonitrile, CH_2Cl_2, and dimethyl sulfoxide were purchased from Fisher Scientific (Hampton, NH). Pooled human liver microsomes, pooled human intestinal microsomes, supersomes of cDNA-expressed CYP enzymes (expressed in baculovirus-insect cells), rat P450 oxidoreductase insect cells,

This work was supported by the National Institutes of Health National Institute of General Medical Sciences [Grant R01 GM25515] (to P.R.O.M.) and the Australian Research Council [Grant DP110104455] (to J.D.V.). H.P. was supported by the National Research Foundation of Korea [Grant 2011-0016509].

An earlier account of this work was presented by Paul R. Ortiz de Montellano at the *18th International Conference on Cytochrome P450 Biochemistry, Biophysics and Biotechnology*, Seattle, Washington, June 19, 2013.

dx.doi.org/10.1124/dmd.114.056903.

[S]This article has supplemental material available at dmd.aspetjournals.org.

ABBREVIATIONS: IPA, isopropanol; LC-MS, liquid chromatography-mass spectrometry; 6-MNA, 6-methoxy-2-naphthylacetic acid; NADPH, β-nicotinamide adenine dinucleotide 2′-phosphate, reduced; αNF, α-naphthoflavone; P450, cytochrome P450; t_R, retention time.

and insect cells were purchased from BD Biosciences (San Jose, CA). The recombinant CYP2C8, -2C9, -2E1, -2J2, -2S1, -2W1, and -3A4 were expressed in *Escherichia coli* and purified with minor modifications according to the published protocols for these proteins (Wang et al., 2001; Wester et al., 2004; Wu et al., 2006; Porubsky et al., 2008; Singh et al., 2008; Messina et al., 2010; Nishida et al., 2010). Recombinant human NADPH-cytochrome P450 reductase (CPR) was expressed in *E. coli* and purified as previously described (Varfaj et al., 2012).

Air-sensitive experiments were conducted under an N_2 or Ar environment using oven-dried glassware. Tetrahydrofuran (THF) was distilled off sodium-benzophenone ketyl while pyridine, CH_2Cl_2 and triethylamine were dried over and distilled from CaH_2. Other anhydrous solvents were dried based on conventional procedures, distilled, and stored under vacuum or N_2 prior to use. Thin layer chromatography was conducted on Kieselgel 60 F_{254} plates (Merck KGaA, Darmstadt, Germany) and visualized by a vanillin dip (6.0 g vanillin in 250 ml EtOH with 2.5 ml concentrated H_2SO_4) or phosphomolybdic acid (5% in EtOH). Flash column chromatography was conducted on Silica gel 60 (0.04–0.06 mm, 230–400 mesh, Merck). Analytical and preparative enantioselective HPLC were performed on an Agilent 1200 series liquid chromatograph (flow rate of 0.5 ml·min^{-1} for analytical, 10 ml·min^{-1} for preparative) equipped with UV (254 nm) and Advanced Laser Polarimeter (PDR-Chiral Inc. Lake Park, Florida) detectors and a Chiralpak IC column (4.6 × 250 mm analytical or 20 × 250 mm preparative, Daicel Chemical Industries Ltd., Osaka, Japan). ^{1}H and ^{13}C NMR spectra were recorded on Bruker AV300, Bruker AV400, or Bruker AV500 spectrometers (Bruker, Billerica, Massachusetts) as stated with signals in part per million (ppm) on the δ scale. The residual solvent peaks served as internal standard ($CDCl_3$: δ_H 7.24 and δ_C 77.0; C_6D_6: δ_H 7.15 and δ_C 128.0; CD_3OD: δ_H 3.30 and δ_C 128.0). Melting points were determined on a DigiMelt MSRS apparatus (Stanford Research Systems, Sunnyvale, California). Gas chromatography-mass spectrometry (GC-MS) analyses were conducted on a Shimadzu GC-MS QP2010-plus apparatus, operating at 70 eV, connected to a GC-2010 gas chromatograph fitted with a DB-5 column (30 m, internal diameter 0.25 mm; J&W Scientific, Folsom, California). Standard GC-MS program was as follows: split mode; column flow 2.72 ml/min; total flow 84.2 ml/min; injector 250°C; detector 250°C; oven 80°C (1.0-minute equilibration) held for 2.0 minutes, ramp 16°C/min to 250°C and held for 30.0 minutes (total program time 42.63 minute). Elemental microanalyses were conducted by Microanalytical Service, School of Chemistry and Molecular Biosciences (University of Queensland). High-resolution mass spectra (HRMS) were recorded on a Bruker micrOTOF-Q spectrometer [positive ion Electrospray ionization (ESI) mode].

Synthesis of Nabumetone Derivatives

3-Hydroxy-4-(6-methoxynaphthalen-2-yl)butan-2-one (2) and 1-Hydroxy-4-(6-methoxynaphthalen-2-yl)butan-2-one (3) and 3-(6-Methoxynaphthalen-2-yl)propanoic acid (4). Freshly distilled triethylamine (0.38 g, 3.74 mmol) was added to a stirred solution of nabumetone (1) (0.50 g, 2.20 mmol) in anhydrous CH_2Cl_2 (5 ml) at 0°C. Trimethylsilyl trifluoromethanesulfonate in CH_2Cl_2 (1 M, 3.74 mmol) was then added dropwise into the reaction mixture. After 15 minutes of stirring, saturated aqueous $NaHCO_3$ (10 ml) was added, followed by additional anhydrous CH_2Cl_2 (5 ml). Then, *meta*-chloroperbenzoic acid (77%, 0.74 g, 3.3 mmol) was added slowly into the reaction flask. After complete addition of *meta*-chloroperbenzoic acid, the water bath was immediately removed and the colorless solution was left to stir for another hour at room temperature. The organic layer was separated and the aqueous layer was extracted with CH_2Cl_2 (5 ml). The combined organic layers were washed with water (10 ml), brine (10 ml), dried ($MgSO_4$), and concentrated in vacuo. The residue was then taken up in THF (7 ml) before *p*-TsOH (84.3 mg, 0.44 mmol) was added slowly into the solution at 0°C. Stirring was continued at room temperature. After 0.5 hour, water (10 ml) was added, and the organic layer was separated. The aqueous layer was extracted with Et_2O (2 × 5 ml), and the combined organic layers were washed with brine (10 ml), dried ($MgSO_4$), and concentrated in vacuo. Purification via column chromatography (silica gel 60, 15% EtOAc in petroleum spirit) gave nabumetone (23%) and hydroxyketones 2 and 3 (Scheme 1) (87% based on recovered starting material) as white solids. Hydroxy-ketone *rac*-2 (0.15 g, 37%). Observed melting point (mp): 105–108.9°C, literature (lit.) (Goudie, 1983) mp: 107–110°C. NMR spectra are identical to the reported data (Nobilis et al., 2013). Hydroxy-ketone 3 (0.21 g, 50%). Observed mp: 107–108°C, lit. (Goudie, 1983) mp: 106–109°C. ^{1}H NMR (500 MHz, $CDCl_3$) δ 2.79 (t, J = 7.9 Hz, 2H, $RCH_2\underline{CH_2}COR'$), 3.08 (t, J = 7.6 Hz, 2H, $RC\underline{H_2}CH_2COR'$), 3.89 (s, 3H, $ArOC\underline{H_3}$), 4.18 (s, 2H, $RCOC\underline{H_2}OH$), 7.08 (d, J = 2.5 Hz, 1H, Ar-$\underline{H}$), 7.11 (dd, J = 8.9, 2.6 Hz, 1H, Ar-$\underline{H}$), 7.25 (dd, J = 7.6, 1.8 Hz, 1H, Ar-$\underline{H}$), 7.52 (s, 1H, Ar-$\underline{H}$), 7.65 (dd, J = 8.4, 4.1 Hz, 2H, Ar-$\underline{H}$). ^{13}C NMR (125 MHz, $CDCl_3$) δ 29.6, 40.0, 55.3, 68.4, 105.6, 119.0, 126.3, 127.1, 127.2, 129.0, 129.0, 133.2, 135.2, 157.4, 208.9. GC-MS *m/z* (%) 244 ($C_{15}H_{16}O_3$·, 24), 172 (13), 171 (100), 141 (17), 128 (34), 115 (21), 43 (12). HRMS ESI calculated (calcd) for $C_{15}H_{16}NaO_3$ ([M+Na]$^+$): 267.0992. Observed: 267.1001.

Analytical and Preparative Enantioselective HPLC of *Rac*-3-hydroxy-4-(6-methoxynaphthalen-2-yl)butan-2-one (*rac*-2). Preparative enantioselective HPLC purification [Chiralpak IC column, isocratic conditions of 45% isopropanol (IPA) in hexane, 10 ml·min^{-1}] was performed with 1.5 ml injections of a 2 mg·ml^{-1} solution of *rac*-2 in 45% IPA in hexane. Retention times were compound (4) 7.7 minutes; *R*-2 11.3 minutes; *S*-2 13.4 minutes. Both enantiomers were obtained enantiomerically pure (>99% *ee*) after preparative HPLC separation, as determined by analytical enantioselective HPLC (Chiralpak IC column, isocratic conditions of 45% IPA in hexane, 0.5 ml·min^{-1}). Retention times were *R*-2, 12.0 minutes; *S*-2, 13.8 minutes. These compounds are spectroscopically identical to *rac*-2 (Nobilis et al., 2013) (*R*)-3-hydroxy-4-(6-methoxynaphthalen-2-yl)butan-2-one (*R*-2), $[\alpha]_D^{25}$ = +20.3 (*c* 0.27, 45% IPA-hexane), $[\alpha]_D^{25}$ = -45.9 (*c* 0.33, $CHCl_3$), HRMS ESI calcd for $C_{15}H_{16}NaO_3$ ([M+Na]$^+$): 267.0992. Observed: 267.0993. (*S*)-3-hydroxy-4-(6-methoxynaphthalen-2-yl)butan-2-one (*S*-2), $[\alpha]_D^{25}$ = -18.5 (*c* 0.27, 45% IPA-hexane), $[\alpha]_D^{25}$ = +38.3 (*c* 0.34, $CHCl_3$), HRMS ESI calcd for $C_{15}H_{16}NaO_3$ ([M+Na]$^+$): 267.0992. Observed: 267.1002. 3-(6-methoxynaphthalen-2-yl) propanoic acid (4) was isolated as a white solid as a minor impurity during preparative enantioselective HPLC. Observed mp: 155.5–157°C, lit. (Jacques and Horeau, 1948) mp: 156–157°C. ^{1}H NMR (500 MHz, C_6D_6) δ 2.40 (t, J = 8.0 Hz, 2H, $RCH_2\underline{CH_2}COOH$), 2.86 (t, J = 7.7 Hz, 2H, $RC\underline{H_2}CH_2COOH$), 3.39 (s, 3H, $ArOC\underline{H_3}$), 6.92 (d, J = 2.5 Hz, 1H, Ar-$\underline{H}$), 7.09 (dd, J = 8.4, 1.8 Hz, 1H, Ar-$\underline{H}$),7.19 (dd, J = 9.0, 2.6 Hz, 1H, Ar-$\underline{H}$), 7.32 (s, 1H, Ar-$\underline{H}$), 7.47 (d, J = 8.4 Hz, 1H, Ar-$\underline{H}$), 7.52 (d, J = 8.4 Hz, 1H, Ar-$\underline{H}$). ^{13}C NMR (125 MHz, C_6D_6) δ 29.8, 34.5, 53.7, 104.9, 118.3, 125.8, 126.3, 126.6, 128.4, 128.7, 132.9, 134.6, 156.9, 176.7. MS ESI: *m/z* 253 ([M+Na]$^+$). HRMS ESI calcd for $C_{14}H_{14}NaO_3$ ([M+Na]$^+$): 253.0835. Observed: 253.0846.

(2′*S*,2*R*)-1′-(6′-methoxynaphthalen-2′-yl)-3′-oxobutan-2′-yl 3,3,3-trifluoro-2-methoxy-2-phenylpropanoate (2′*S*,2*R*-10) and (2′*R*,2*R*)-1′-(6′-methoxynaphthalen-2′-yl)-3′-oxobutan-2′-yl 3,3,3-trifluoro-2-methoxy-2-phenylpropanoate (2′*R*,2*R*-10). To a solution of the second eluting (Chiralpak IC column) enantiomer of 2 (5 mg, 0.02 mmol) in anhydrous CH_2Cl_2 (375 μl) was added 4-dimethylaminopyridine (9.8 mg, 0.08 mmol), N,N'-dicyclohexylcarbodiimide (DCC) (16.6 mg, 0.08 mmol), and (*R*)-methoxy(trifluoromethyl)phenylacetic acid (18.7 mg, 0.08 mmol). The resulting solution was left to stir at room temperature overnight. After filtration and removal of solvent, the crude was purified via column chromatography (silica gel 60, 15% EtOAc in petroleum spirit) to give (2′*S*,2*R*)-1′-(6′-methoxynaphthalen-2′-yl)-3′-oxobutan-2′-yl 3,3,3-trifluoro-2-methoxy-2-phenylpropanoate (2′*S*,2*R*-10) (6.8 mg, 74%) as a white amorphous solid. ^{1}H NMR (400 MHz, $CDCl_3$) δ 2.12 (s, 3H, $RCOC\underline{H_3}$), 3.13 (dd, J = 14.4, 9.6 Hz, 1H, $RC\underline{H_2}R'$), 3.31 (m, 3H, $ROC\underline{H_3}$), 3.34 (dd, J = 14.5, 4.0 Hz, 1H, $RC\underline{H_2}R'$), 3.92 (s, 3H, $ArOC\underline{H_3}$), 5.46 (dd, J = 9.7, 4.0 Hz, 1H, $RC\underline{H}OR'$), 7.05 (td, J = 7.5, 1.0 Hz, 2H, Ar-$\underline{H}$), 7.11 (d, J = 2.5 Hz, 1H, Ar-$\underline{H}$), 7.13 (dd, J = 8.8, 2.6 Hz, 1H, Ar-$\underline{H}$), 7.19 (d, J = 7.9 Hz, 2H, Ar-$\underline{H}$), 7.24 (td, J = 7.4, 1.2 Hz, 1H, Ar-$\underline{H}$), 7.27 (dd, J = 8.4, 1.8 Hz, 1H, Ar-$\underline{H}$), 7.56 (s, 1H, Ar-$\underline{H}$), 7.61 (d, J = 8.9 Hz, 1H, Ar-$\underline{H}$), 7.66 (d, J = 8.4 Hz, 1H, Ar-$\underline{H}$). ^{13}C NMR (100 MHz, $CDCl_3$) δ 26.5, 36.6, 55.3, 81.4, 84.5 (q, $J_{C\text{-}CF3}$ = 27.8 Hz), 105.6, 119.2, 123.1 (q, $J_{C\text{-}F}$ = 286.7 Hz), 127.3, 127.3, 127.6, 128.2, 128.2, 128.9, 129.2, 129.5, 130.3, 131.5, 133.7, 157.8, 166.3, 203.5. MS ESI: *m/z* 483 ([M+Na]$^+$). HRMS ESI calcd for $C_{29}H_{28}NaO_5$ ([M+Na]$^+$): 483.1395. Observed: 483.1392.

The method above was used with the first eluting (Chiralpak IC column) enantiomer of 2 (2 mg, 0.0082 mmol) to prepare (2′*R*,2*R*)-1′-(6′-methoxynaphthalen-2′-yl)-3′-oxobutan-2′-yl 3,3,3-trifluoro-2-methoxy-2-phenylpropanoate (2′*R*,2*R*-10) (0.6 mg, 16%) as a white amorphous solid. ^{1}H NMR (400 MHz, $CDCl_3$) δ 2.14 (s, 3H, $RCOC\underline{H_3}$), 3.13 (dd, J = 14.4, 8.6 Hz, 1H, $RC\underline{H_2}R'$), 3.28 (dd, J = 14.5, 4.5 Hz, 1H, $RC\underline{H_2}R'$), 3.48 (m, 3H, $ROC\underline{H_3}$), 3.91 (s, 3H, $ArOC\underline{H_3}$), 5.47 (dd, J = 8.5, 4.5 Hz, 1H, $RC\underline{H}OR'$), 7.06 (d, J = 2.5 Hz, 1H, Ar-$\underline{H}$), 7.10 (dd, J = 8.9, 2.5 Hz, 1H, Ar-$\underline{H}$), 7.15 (dd, J = 8.4, 1.8 Hz, 1H, Ar-$\underline{H}$), 7.17 (td, J = 7.8, 1.4 Hz, 2H, Ar-$\underline{H}$), 7.26 (td, J = 7.4, 1.1 Hz, 1H, Ar-$\underline{H}$), 7.37 (d,

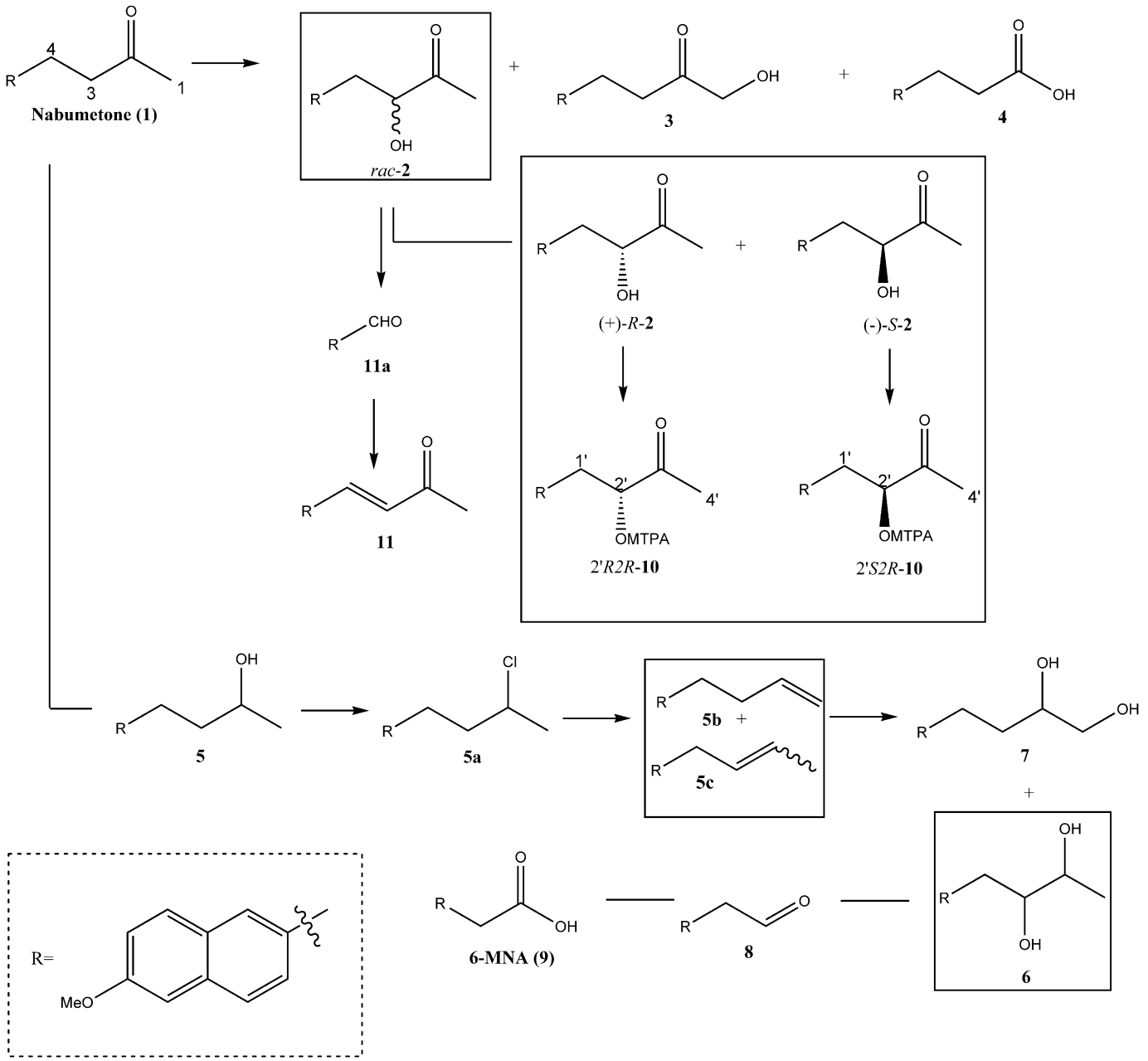

Scheme 1. Schematic outline of the synthesis of nabumetone derivatives (2–11) from nabumetone (1). The numbers below each structure indicate their compound number, which corresponds to the following structural names: 1, 4-(6-methoxynaphthalen-2-yl)butan-2-one; 2,3-hydroxy-4-(6-methoxynaphthalen-2-yl)butan-2-one; (+)-*R*-2, (3*R*)-3-hydroxy-4-(6-methoxynaphthalen-2-yl)butan-2-one; (−)-*S*-2, (3*S*)-3-hydroxy-4-(6-methoxynaphthalen-2-yl)butan-2-one; 3,1-hydroxy-4-(6-methoxynaphthalen-2-yl)butan-2-one; 4,3-(6-methoxynaphthalen-2-yl)propanoic acid; 5,4-(6-methoxynaphthalen-2-yl)butan-2-ol; 5a, 2-(3-chlorobutyl)-6-methoxynaphthalene; 5b, 2-(but-3-enyl)-6-methoxynaphthalene; 5c, (*E*)- and (*Z*)-2-(but-2-en-1-yl)-6-methoxynaphthalene mixture; 6,1-(6-methoxynaphthalen-2-yl)butane-2,3-diol; 7,4-(6-methoxynaphthalen-2-yl) butane-1,2-diol; 8, (6-methoxynaphthalen-2-yl)acetaldehyde; 9, (6-methoxynaphthalen-2-yl)acetic acid; 2′*R*2*R*-10, (2′*R*,2*R*)-1′-(6′-methoxynaphthalen-2′-yl)-3′-oxobutan-2′-yl 3,3,3-trifluoro-2-methoxy-2-phenylpropanoate; 2′*S*,2*R*-10, (2′*S*,2*R*)-1′-(6′-methoxynaphthalen-2′-yl)-3′-oxobutan-2′-yl 3,3,3-trifluoro-2-methoxy-2-phenylpropanoate; 11a, 6-methoxy-2-naphthaldehyde; 11, (3*E*)-4-(6-methoxynaphthalen-2-yl)but-3-en-2-one. Synthesis of these compounds is described in *Materials and Methods*.

J = 8.0 Hz, 2H, Ar-H), 7.43 (s, 1H, Ar-H), 7.53 (d, *J* = 9.0 Hz, 1H, Ar-H), 7.57 (d, *J* = 8.4 Hz, 1H, Ar-H). ^{13}C NMR (100 MHz, $CDCl_3$) δ 27.1, 36.5, 55.3, 80.9, 105.5, 119.0, 127.2, 127.3, 127.5, 128.0, 128.3, 128.8, 129.2, 129.5, 130.0, 131.6, 133.6, 157.7, 166.3, 203.3 (C-CF_3 quartets were not observed because of signal to noise). MS ESI: *m/z* 483 ($[M+Na]^{+\cdot}$). HRMS ESI calcd for $C_{29}H_{28}NaO_5$ ($[M+Na]^{+\cdot}$): 483.1395. Observed: 483.1391.

1-(6-Methoxynaphthalen-2-yl)butane-2,3-diol (6) and 4-(6-Methoxynaphthalen-2-yl)butane-1,2-diol (7). $POCl_3$ (1.65 g, 10.95 mmol) was added dropwise to a solution of 5 (Goudie et al., 1978) (250 mg, 1.09 mmol) in pyridine (7.5 ml) at 0°C for over a period of 40 minutes. The resulting solution was allowed to warm to room temperature and stirred overnight. The reaction mixture was diluted with EtOAc (50 ml) before it was poured slowly into a mixture of 4 M HCl (25 ml) and crushed ice (50 g). The organic layer was separated, and the aqueous layer was extracted with EtOAc (25 ml). The combined organic layers were washed with brine (2 × 25 ml) and dried ($MgSO_4$) before solvent was removed in vacuo to give 2-(3-chlorobutyl)-6-methoxynaphthalene (5a) (235 mg, 87%) as a white solid. Observed mp: 58–59°C. ^{1}H NMR (300 MHz, $CDCl_3$) δ 1.53 (d, *J* = 6.6 Hz, 3H, RCHClCH_3), 2.02–2.11 (m, 2H, RCH_2CHClCH_3), 2.80–3.02 (m, 2H, RCH_2CH_2CHClR′), 3.90 (s, 3H, ArOCH_3), 4.00 (m, 1H, RCHClCH_3), 7.10–7.13 (m, 2H, Ar-H), 7.28 (dd, *J* = 8.4, 1.7 Hz, 1H, Ar-H), 7.55 (s, 1H, Ar-H), 7.66 (d, *J* = 8.3 Hz, 2H, Ar-H). ^{13}C NMR (75 MHz, $CDCl_3$) δ 25.4, 32.8, 41.9, 55.3, 57.9, 105.6, 118.8, 126.5, 126.9, 127.7, 128.9, 129.1,

133.1, 136.2, 157.3. GC-MS *m/z* (%) 248 ($C_{15}H_{17}ClO^{\cdot}$, 22), 171 (100), 172 (19), 141 (12), 129 (11), 128 (57), 115 (17), 127 (12), 102 (12), 63 (29), 51 (11), 42 (12), 41 (50), 40 (7). combustion elemental analysis (Anal.) calcd: C, 72.43; H, 6.89. Found: 72.45; H, 6.93.

A solution of 5a (407 mg, 1.64 mmol) in NaOEt in EtOH (3.6 M, 40 mmol) was subsequently heated at reflux overnight. The mixture was quenched with addition of H_2O (70 ml). The products were then extracted into Et_2O (3 × 20 ml), and the combined organic layers were washed with brine (2 × 25 ml) and dried ($MgSO_4$) before the solvent was removed in vacuo. Purification via column chromatography (silica gel 60, 3% Et_2O in petroleum spirit) afforded a mixture of 2-(but-3-enyl)-6-methoxynaphthalene (5b), (*E*)-2-(but-2-en-1-yl)-6-methoxynaphthalene (*E*-5c) and (*Z*)-2-(but-2-en-1-yl)-6-methoxynaphthalene (*Z*-5c) (4:4:1 ratio based on NMR integration) as a white solid (230 mg, 68%). ^{1}H NMR (500 MHz, $CDCl_3$) δ 1.69 (dq, J = 6.3, 1.4 Hz, RCH=CHC$\underline{H}_3$, *E*-5c), 1.75 (broad d, J = 5.3 Hz, RCH=CHC$\underline{H}_3$, *Z*-5c), 2.43 (m, J = 7.6 Hz, RC$\underline{H}_2$C$\underline{H}_2$CH=CH$_2$, 5b), 2.82 (t, J = 7.8 Hz, RC$\underline{H}_2$CH$_2$CH=CH$_2$, 5b), 3.42 (broad d, J = 6.6 Hz, RC$\underline{H}_2$CH=CHR′, *E*-5c), 3.51 (broad d, J = 6.0 Hz, RC$\underline{H}_2$CH=CHR′, *Z*-5c), 3.89–3.90 (overlapping s, ArOC$\underline{H}_3$), 4.97 (m, J = 10.3 Hz, RCH=C$\underline{H}_2$, 5b), 5.04 (dq, J = 17.0, 1.7 Hz, RCH=C$\underline{H}_2$, 5b), 5.53 (dqt, J = 15.1, 4.2, 1.3 Hz, RCH=C$\underline{H}$CH$_3$, *E*-5c), 5.63 (dtq, J = 14.9, 3.3, 1.5 Hz, RC$\underline{H}$=CHCH$_3$, *E*-5c), 5.49–5.67 (overlapping m, RC$\underline{H}$=C$\underline{H}$CH$_3$, *Z*-5c), 5.87 (ddt, J = 17.0, 10.3, 6.6 Hz, 1H, RC$\underline{H}$=CH$_2$, 5b), 7.07–7.13 (m, Ar-$\underline{H}$), 7.25–7.31 (m, Ar-$\underline{H}$), 7.50–7.55 (m, Ar-$\underline{H}$), 7.63–7.68 (m, Ar-$\underline{H}$). 5b. GC-MS *m/z* (%) 212 ($C_{15}H_{16}O^{\cdot}$, 20), 172 (13), 171 (100), 128 (48), 115 (10), 102 (7), 41 (38). *E*-5c and *Z*-5c. GC-MS *m/z* (%) 212 ($C_{15}H_{16}O^{\cdot}$, 100), 197 (67), 182 (21), 181 (20), 171 (20), 166 (18), 165 (64), 153 (31), 152 (25), 141 (21), 139 (20), 129 (14), 128 (64), 127 (15), 115 (38), 77 (15), 63 (21), 51 (14), 45 (29), 41 (43).

N-methylmorpholine-*N*-oxide (26 mg, 0.22 mmol) was added to a stirred solution of the above alkene mixture 5b, 5c (18 mg, 0.086 mmol) in *t*-BuOH/THF/H_2O (10:3:1, 1.7 ml). Then, 0.1 M OsO_4 (86 μl) in *t*-BuOH solution was added, and the resulting clear pale yellow solution was stirred at room temperature overnight before 5% sodium sulfite solution (6 ml) was added and the mixture was stirred vigorously for another 30 minutes. The reaction mixture was extracted into CH_2Cl_2 (3 × 5 ml). The combined organic layer was washed sequentially with water (10 ml) and brine (10 ml) and then dried ($MgSO_4$) before solvent was removed in vacuo. Purification via column chromatography (silica gel 60, 25% EtOAc in petroleum spirit) separated the two desired diols as white solids. 1-(6-Methoxynaphthalen-2-yl)butane-2,3-diol (6) (11.5 mg, 54%). Observed mp: 90–92°C, ^{1}H NMR (300 MHz, $CDCl_3$) δ 1.27 (d, J = 6.2 Hz, 3H, RCHOHC$\underline{H}_3$), 2.80 (dd, J = 13.8, 8.7 Hz, 1H, RC$\underline{H}_2$CHOHR′), 3.01 (dd, J = 13.8, 4.0 Hz, 1H, RC$\underline{H}_2$CHOHR′), 3.63–3.77 (m, 2H, RC$\underline{H}$OHR′), 3.90 (s, 3H, ArOC$\underline{H}_3$), 7.12–7.15 (m, 2H, Ar-$\underline{H}$), 7.32 (dd, J = 8.4, 1.8 Hz, 1H, Ar-$\underline{H}$), 7.60 (s, 1H, Ar-$\underline{H}$), 7.67 (d, J = 8.7 Hz, 1H, Ar-$\underline{H}$), 7.70 (d, J = 8.3 Hz, 1H, Ar-$\underline{H}$). ^{13}C NMR (75 MHz, $CDCl_3$) δ 19.6, 40.0, 55.3, 70.0, 76.6, 105.6, 119.0, 127.2, 127.8, 128.1, 129.0, 129.1, 133.0, 133.4, 157.5. GC-MS *m/z* (%) 246 ($C_{15}H_{18}O_3^{\cdot}$, 11), 212 (9), 197 (7), 172 (33), 171 (59), 165 (7), 158 (7), 157 (7), 141 (8), 129 (13), 128 (47), 115 (25), 102 (11), 77 (7), 63 (17), 45 (100), 43 (30). HRMS ESI calcd for $C_{15}H_{18}NaO_3$ ($[M+Na]^{+\cdot}$): 269.1154. Observed: 269.1153. Anal. calculated: C, 73.15; H, 7.37. Found: 73.09; H, 7.46. 4-(6-methoxynaphthalen-2-yl)butane-1,2-diol (7) (8.2 mg, 39%). Observed mp: 119–121°C. ^{1}H NMR (300 MHz, $CDCl_3$) δ 1.77–1.88 (m, 2H, RC$\underline{H}_2$CHOHR′), 2.76–2.99 (m, 2H, RC$\underline{H}_2$CH$_2$CHOHR′), 3.47 (dd, J = 11.0, 7.5 Hz, 1H, RC$\underline{H}_2$OH), 3.66 (dd, J = 11.8, 3.1 Hz, 1H, RC$\underline{H}_2$OH), 3.70–3.79 (m, 1H, RC$\underline{H}$OHR′), 3.89 (s, 3H, ArOC$\underline{H}_3$), 7.09–7.13 (m, 2H, Ar-$\underline{H}$), 7.29 (dd, J = 8.3, 1.8 Hz, 1H, Ar-$\underline{H}$), 7.55 (s, 1H, Ar-$\underline{H}$), 7.65 (d, J = 8.8 Hz, 2H, Ar-$\underline{H}$). ^{13}C NMR (75 MHz, $CDCl_3$) δ 31.7, 34.6, 55.3, 66.8, 71.5, 105.7, 118.8, 126.3, 126.9, 127.7, 128.9, 129.1, 133.0, 136.8, 157.2. GC-MS *m/z* (%) 246 ($C_{15}H_{18}O_3^{\cdot}$, 22), 196 (8), 172 (31), 171 (100), 165 (7), 141 (11), 129 (8), 128 (84), 127 (18), 115 (24), 102 (10), 77 (12), 73 (38), 63 (13), 55 (14), 45 (9), 44 (32), 43 (56), 42 (28), 41 (50). HRMS ESI calcd for $C_{15}H_{18}NaO_3$ ($[M+Na]^{+\cdot}$): 269.1154. Observed: 269.1159. Anal. calcd: C, 73.15; H, 7.37. Found: 72.90; H, 7.39.

2-(6-Methoxynaphthalen-2-yl)acetaldehyde (8). A solution of $NaIO_4$ (154 mg, 0.71 mmol) in water (5 ml) was added dropwise to a stirred solution of diol 6 (87 mg, 0.35 mmol) in CH_2Cl_2 (5 ml) at 0°C, over a period of 20 minutes. The resulting solution was stirred vigorously at room temperature for 4.5 hours. Then, water (10 ml) was added and the organic layer was separated. The aqueous layer was extracted with CH_2Cl_2 (2 × 10 ml). The combined organic layers were washed with brine (10 ml), dried ($MgSO_4$), and concentrated in vacuo. Purification via column chromatography (silica gel 60, 15% EtOAc in petroleum spirit) afforded 2-(6-methoxynaphthalen-2-yl)acetaldehyde (8) (Pataki et al., 1989) as a white solid (64 mg, 0.32 mmol, 91%). Observed mp: 71–73°C, lit. (Pataki et al., 1989) mp: 70–2°C. 6-Methoxy-2-naphthylacetic acid (6-MNA) (9) could be obtained from further oxidation of 2-(6-methoxynaphthalen-2-yl) acetaldehyde (8). However, in this study we used the commercially available compound (Cayman Chemical Company).

(*E*)-4-(6-methoxynaphthalen-2-yl)but-3-en-2-one (*E*-11). A mixture of *rac*-2 and $Cu(OAc)_2{\cdot}H_2O$ in 2:1 ethanol:H_2O (5.2 ml) solution was stirred at 60°C for 5 hours. After cooling, the solvent was removed in vacuo, and the crude product was diluted with EtOAc (5 ml). The organic layer was washed with $NaHCO_3$ (5 ml) and brine (5 ml) and dried ($MgSO_4$) and concentrated in vacuo. Purification via column chromatography (silica gel 60, 15% EtOAc in petroleum spirit) afforded 6-methoxy-2-naphthaldehyde (11a) (Schmidt et al., 2005) (13.2 mg, 40%).

To a solution of 11a (12 mg, 0.065 mmol) in acetone (300 μl) was added 5% aqueous NaOH (16 μl), and the resulting mixture was stirred overnight at room temperature. The solvent was concentrated under a stream of N_2, and the residue was diluted with water (0.5 ml) before aqueous HCl (1 M) was added until the mixture was acidic. Then, the mixture was extracted with Et_2O (2 × 1 ml), dried ($MgSO_4$), and concentrated in vacuo. Purification via column chromatography (silica gel 60, 10% EtOAc in petroleum spirit) afforded (*E*)-4-(6-methoxynaphthalen-2-yl)but-3-en-2-one (*E*-11) (Viviano et al., 2011) (7.5 mg, 51%) as a yellow solid. Observed mp: 114–115°C, lit. (Goudie et al., 1978) mp: 118–120°C.

Expression and Purification of CYP1A2

The recombinant CYP1A2 protein containing a C-terminal $(His)_5$ tag was expressed and purified as previously described (Kim et al., 2008). Briefly, the pCWori plasmid containing the CYP1A2 gene was transformed into *E. coli* DH5α cells, and a single colony was inoculated in Terrific Broth medium (Fisher Scientific, Waltham, Massachusetts) supplemented with glycerol (0.4% v/v), 1 mM thiamine, 100 μg/ml ampicillin, and trace metals at 37°C. Once cells reached an Abs_{600} value of 0.5–0.8, protein expression was induced by addition of 1 mM isopropyl 1-thio-β-D-galactopyranoside and 0.5 mM 5-aminolevulinic acid and incubated at 30°C for an additional 48 hours. The cells were harvested, lysed, and the spheroplasts containing the CYP1A2 were extracted. Spheroplasts were later solubilized and centrifuged, and the supernatant was loaded onto a HisTrap affinity column (Qiagen, Venlo, The Netherlands). The CYP1A2 purification protocol was similar to that described previously (Kim et al., 2008), except that the α-naphthoflavone (αNF) inhibitor was omitted throughout the procedure. The protein was purified by HisTrap affinity column followed by Q-Sepharose anion exchange chromatography. The eluted CYP1A2 protein was concentrated using 30 kDa Molecular Weight Cut Off concentrators (Millipore, Billerica, Massachusetts) and further dialyzed against 0.1 M potassium phosphate, pH 7.4, buffer containing 20% glycerol. The protein was subject to electrophoresis on a 4–12% SDS-polyacrylamide gel, which was visualized by SimplyBlue gel staining (Invitrogen, Carlsbad, California) and was determined to be greater than 80% pure.

Characterization of CYP1A2

The P450 activity and the concentration of CYP1A2 were determined as previously described (Guengerich et al., 2009). Briefly, formation of the ferrous-CO complex was achieved by bubbling CO gas (Airgas, San Francisco, CA) into the ferric CYP1A2 enzyme solution for 1 minute through a septum-sealed cuvette prior to the injection of 1 mM sodium dithionite using a gas tight syringe (Hamilton, Reno, NV). Differential spectra were generated by subtracting the spectrum of the ferrous deoxy form from that of its carbon monoxide complex, and the concentration of P450 was determined using an extinction coefficient of 91,000 $M^{-1}{\cdot}cm^{-1}$. The presence of heme-bound CYP1A2 was confirmed by pyridine hemochrome assay (Berry and Trumpower, 1987). The catalytic activity of CYP1A2 was assayed by monitoring the *O*-deethylation of 7-ethoxyresorufin by fluorescence (Kim et al., 2008). Briefly, reaction mixtures contained 100 pmol CYP1A2, 200 pmol CPR, 30 μg L-α-dilauroyl-*sn*-glycero-3-phosphocholine (DLPC) and substrate concentrations of 20 and 50 μM in 0.1 M potassium phosphate buffer, pH 7.4, in a total volume of 0.5 ml. The reaction was initiated by addition of the NADPH-generating system

(0.5 mM $NADP^+$, 10 mM glucose-6-phosphate, and 1.0 IU glucose-6-phosphate dehydrogenase, and $MgCl_2$) into the mixture, which was later incubated for 10 minutes at 37°C prior to termination by addition of 200 μl of methanol. The catalytic activity of CYP1A2 was also determined by monitoring the *O*-deethylation of phenacetin, with phenacetin at a concentration of 0.2 mM (Yun et al., 2000). The His_5-tag at the C terminus of CYP1A2 has been shown not to affect the enzyme's catalytic activity (Yun et al., 2000).

Nabumetone Metabolism

The incubation mixtures in 0.1 M potassium phosphate, pH 7.4, buffer contained an NADPH-generating system (0.5 mM $NADP^+$, 4 mM glucose-6-phosphate, 4.0 U/ml glucose-6-phosphate dehydrogenase, and 5 mM $MgCl_2$), 45 μM DLPC, 25 μg/ml catalase, 0.3 μM CYP1A2, 0.6 μM human CPR, and 0.2 mM nabumetone. The nabumetone in acetonitrile was added to the reaction mixture to a final acetonitrile concentration of 0.5% v/v, which has a minimal effect on CYP1A2 catalytic activity. The reaction mixture (200 μl) was preincubated for 2 minutes in a 37°C water bath, and then metabolism was initiated by addition of the CYP1A2. Control reactions omitted either CYP1A2 or the CPR/NADPH-generating system. The reaction mixture was incubated for 60 minutes before it was terminated by the addition of ice-cold acetonitrile/formic acid to a final concentration of 33% acetonitrile/0.1% formic acid. The samples were then cooled on ice to precipitate the proteins before the mixture was vortex-mixed and spun at 10,000 *g* for 3 minutes. The supernatant containing the extracted analytes was loaded onto a liquid chromatography system for further analysis.

Nabumetone Metabolism using Peroxide Shunt Pathway

The reaction mixture contained 0.2 mM of either nabumetone or 3-hydroxynabumetone as the substrate, 45 μM DPLC, and 1 mM cumene hydroperoxide, all in 0.1 M potassium phosphate, pH 7.4 buffer. The reaction was initiated by addition of either CYP1A2 (0.5 mM) or CYP3A4 (0.5 mM). Control experiments lacked either the P450 enzyme or cumene hydroperoxide. In addition, shunt reactions were also run in the presence of the free radical scavengers ascorbic acid (1 mM) or butylated hydroxytoluene (2 mM) to evaluate the possible role of free radicals in the observed reaction. The reactions were incubated for up to 60 minutes at 37°C and terminated, extracted, and analyzed as described above for the nabumetone metabolism reactions.

HPLC and MS Analysis

Samples were first analyzed by injection (50 μl) onto a reverse-phase ^{18}C column (4.6 × 150 mm, 5 μm, Agilent Eclipse XDB) on an Agilent 1200 HPLC connected to a UV diode array detector and a fluorescence detector. Detection of metabolites was performed in the UV-visible range at 229 nm and by fluorescence at 355 nm with excitation at 280 nm. Separation of analytes was achieved by isocratic elution with 40% acetonitrile/0.1% formic acid (0–12 minutes), followed by a linear gradient of 40–100% acetonitrile/0.1% formic acid in H_2O/0.1% formic acid (12–38 minutes) at an eluent flow rate of 0.5 ml/min.

Identification of the metabolites was accomplished by liquid chromatography-mass spectrometry (LC-MS) on a Waters Micromass ZQ (Waters, Milford, Massachusetts) coupled to a Waters Alliance HPLC equipped with a 2695 separations module, a Waters 2487 Dual λ Absorbance detector, and a reverse-phase C_{18} column (4.6 × 150 mm, 5 μm, Agilent Eclipse XDB). The mass spectrometer was operated in the positive ion mode using electrospray (ES) to monitor the precursor to product ion transition of *m/z* 229.3 → 171.1 for nabumetone and 217.3 → 171.1 for 6-MNA, as previously published (Patel et al., 2008). Nabumetone and its derivatives were analyzed using the total ion current signal and the extracted ion for the specific mass. The mass spectrometer settings were as follows: mode, ES^+; capillary voltage, 3.5 kV; cone voltage, 20 V; desolvation temperature, 250°C. The UV absorbance at 229 nm and MS ES^+ spectra were recorded simultaneously.

Results

Potential Nabumetone Metabolites

The key metabolic intermediate, 3-hydroxynabumetone (2), was synthesized *via* epoxidation of the trimethylsilyl enol ether of nabumetone (1) followed by acid catalyzed hydrolysis (Scheme 1). Both the 1- and 2-silyl enol ethers were formed upon treatment of nabumetone (1) with trimethylsilyl trifluoromethanesulfonate in the presence of triethylamine. Thus, after epoxidation with *m*-CPBA and acid hydrolysis, both 3-hydroxy- (2) and 1-hydroxynabumetone (3) were formed in good yield (37 and 50%, respectively) and were easily separated via column chromatography. Recently, 2 was synthesized via α-bromination of nabumetone (1) (Nobilis et al., 2013) and subsequent silver-assisted hydrolysis of the 3-bromonabumetone produced. The overall yield of this process (27%) was less than reported here. Preparative enantioselective HPLC (Chiralpak IC column) was used to resolve racemic 2 to afford pure *R*-2 and *S*-2 (>99% *ee*). Analysis of the corresponding Mosher's esters was then undertaken to assign the absolute configuration of the separated enantiomers. Both *R*-2 and *S*-2 were converted to their *R*-(*R*)-methoxy(trifluoromethyl)phenylacetic acid ester, respectively, 2′*R*,2*R*-10 and 2′*S*,2*R*-10. Based upon ^1H NMR data, the diagnostic $\Delta\delta^{SR}$ of (2′*R*,2*R*)-10 and (2′*S*,2*R*)-10, were calculated (Supplemental Fig. 1) and, following Mosher's model (Dale and Mosher, 1973), the absolute stereochemistry of the first and second eluting enantiomers of 2 was established as *R* and *S*, respectively. Interestingly, the $\Delta\delta^{SR}$ of the methoxy group in 10 was quite large (±0.165). This has previously been attributed to the presence of an additional aromatic moiety on the alcohol providing an extra anisotropic effect (Kelly, 1999).

Other potential intermediates in P450-mediated cleavage of the nabumetone side chain, diols 6 and 7, were accessible from the known 5 (Goudie et al., 1978) in three steps. Treatment of 5 with $POCl_3$ in pyridine gave the corresponding chloride 5a, and subsequent sodium ethoxide-mediated elimination yielded the alkenes 5b, *E*-5c, and *Z*-5c as a mixture in a 4:4:1 ratio. Osmium tetroxide-mediated dihydroxylation under Upjohn conditions (Vanrheenen et al., 1976) gave pure 6 and 7 after chromatography (54 and 39% yield, respectively).

Aldehyde 8 (Pataki et al., 1989) was prepared via oxidative cleavage of 6 with $NaIO_4$ in 91% yield. Finally, the alkene *E*-11 (Viviano et al., 2011) was synthesized from aldehyde 11a (Schmidt et al., 2005) via an aldol reaction with acetone as described in the literature (Goudie et al., 1978). Interestingly, we had observed 11a as a significant product during attempted oxidation of 2 under a variety of conditions and thus used 2 as a precursor for 11a.

Nabumetone Oxidation by Recombinant CYP1A2

Recombinant, reconstituted CYP1A2 (0.3 μM) was used rather than cDNA expressed CYP1A2 supersomes (BD Biosciences) for studies of the oxidation of nabumetone (0.2 mM), because it minimized alternative reactions catalyzed by other enzymes. Control experiments with liver microsomes lacking CYP1A2 and CPR revealed significant reduction of nabumetone (1) to 2-hydroxynabumetone (5), in line with the recent demonstration that several enzymes in both liver microsomes and cytosol can reduce the nabumetone carbonyl group (Skarydova et al., 2013).

To determine whether metabolites were produced by recombinant CYP1A2, control experiments were performed in which either the CPR/NADPH-generating system was omitted or αNF, a reversible CYP1A2 inhibitor, was added at a concentration of 1 μM (K_i = 1–50 nM) (Cho et al., 2003). The control done in the absence of CPR/NADPH-generating system deprives P450 enzyme of the electrons necessary for performing its substrate oxidation, whereas the control in the presence of αNF inhibitor significantly decreases CYP1A2-catalyzed product formation. HPLC analysis of the nabumetone oxidation reaction revealed the generation of several metabolites labeled M1 to M8 (Fig. 1). The identity of these metabolites was established by LC-MS analysis and by comparison of their retention time and mass spectra with those of authentic standards (Scheme 1).

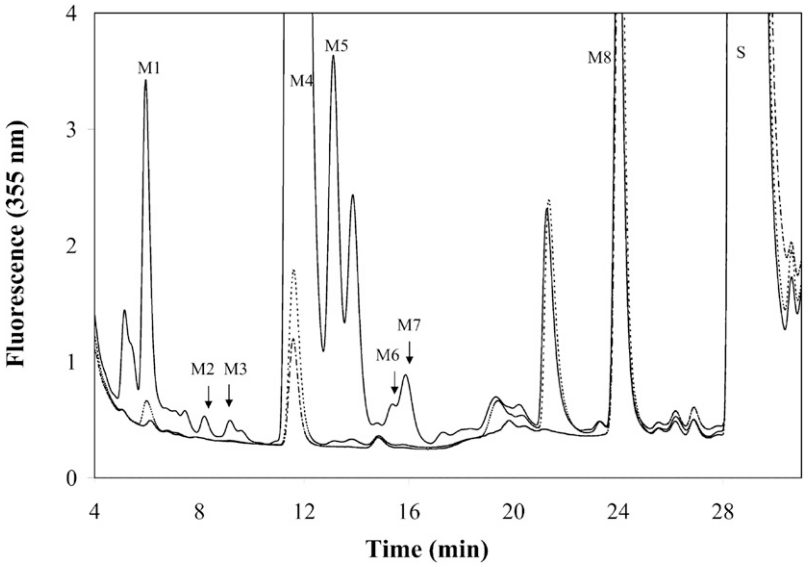

Fig. 1. Reverse-phase (RP)-HPLC separation of the CYP1A2-catalyzed oxidation products of nabumetone (1). The continuous line shows the regular enzymatic reaction, the dashed line shows the control reaction done in the absence of CPR/NADPH-generating system, and the dotted line shows the control done in the presence of the CYP1A2 inhibitor αNF. The reactions were set up and analyzed as described in *Materials and Methods*. The elution was monitored by fluorescence at 355 nm and absorbance at 229 nm. The fluorescence data are generally shown in the figures because the signal-to-noise ratio was better. The metabolites formed are labeled M1–M8 and the substrate nabumetone (1) as S. Their chromatographic identification numbers, compound numbers, retention times, molecular masses, and *m/z* parent ions are summarized in Table 1.

The metabolites identified, their peak number, retention time (t_R), molecular weight, and parent ion mass are summarized in Table 1. An additional major peak for a metabolite with an HPLC retention time of 11.7 minutes was found that did not coincide with any of the authentic standards.

A nabumetone concentration of 0.2 mM ($\sim 4.5 \times K_m$) was used in this study based on the K_m value of nabumetone for CYP1A2. The K_m was determined by setting up the reactions with a CYP1A2 concentration of 0.3 μM and concentrations of nabumetone ranging from 10 to 1000 μM. The 6-MNA product formed was plotted against the concentration of nabumetone in each incubation, and the data were fitted to the Michaelis-Menten equation (Supplemental Fig. 2). The K_m obtained was 47 μM, a value similar to the previously reported value of 45 μM (Turpeinen et al., 2009).

Catalytic Turnover of Possible Intermediates by Recombinant CYP1A2

To elucidate the pathway for the conversion of nabumetone to 6-MNA by CYP1A2, we examined the oxidation of several intermediates (0.2 mM) that, based on the products detected or theoretical considerations, might be formed during the catalytic oxidation of nabumetone: (+)-3-hydroxynabumetone [(+)-*R*-2] (Fig. 2), (−)-3-hydroxynabumetone [(−)-*S*-2], 1-hydroxynabumetone (3), 4-(6-methoxynaphthalen-2-yl)butan-2-ol (5), 4-(6-methoxy-naphthalen-2-yl)butane-2,3-diol (6) (Fig. 3), 4-(6-methoxynaphthalen-2-yl)butane-1,2-diol (7), and 2-(6-methoxynaphthalen-2-yl)acetaldehyde (8) (Fig. 4). Control reactions were also performed with αNF present to inhibit CYP1A2 or with omission of the CPR/NADPH-generating system. The results showed that CYP1A2 forms 6-MNA in highest amount from the aldehyde precursor, 2-(6-methoxynaphthalen-2-yl)acetaldehyde (8), followed in decreasing order from (+)-3-hydroxynabumetone (*R*-2), (−)-3-hydroxynabumetone (*S*-2), and finally nabumetone (1) itself (Fig. 5). CYP1A2 oxidized both (+)-3-hydroxynabumetone and (−)-3-hydroxynabumetone to 6-MNA, with the former consistently being a slightly better substrate in each independent experiment (Fig. 5). CYP1A2 is thus modestly enantioselective in this reaction. The 6-MNA observed in the control reactions (Fig. 2) is an impurity left from (+)-3-hydroxynabumetone preparation.

The oxidation of 4-(6-methoxynaphthalen-2-yl)butane-2,3-diol (6) by CYP1A2 yielded 3-hydroxynabumetone (2) (Fig. 3), demonstrating that CYP1A2 can convert the C2-hydroxyl group to a ketone, a transformation also observed with 4-(6-methoxynaphthalen-2-yl)butane-1,2-diol (7) and 4-(6-methoxynaphthalen-2-yl)butan-2-ol (5) (data not shown). In addition to forming 3-hydroxynabumetone (2), oxidation of the 2,3-diol (6) produces lower yields of 6-MNA (9), a finding entirely consistent with CYP1A2-catalyzed oxidation of the 2,3-diol (6) to the 2-keto-3-alcohol (2) followed by normal cleavage to 6-MNA (9).

The oxidation of nabumetone (1) (t_R = 28.7 minutes), in addition to forming 3-hydroxynabumetone (2) (t_R = 15.8 minutes), also forms

TABLE 1

Summary of metabolites formed from CYP1A2-catalyzed oxidation of nabumetone (1) (Fig. 1)

Chromatographic identification numbers, compound numbers, retention times, molecular weights, and masses of the parent ions are listed. The metabolites were separated and identified by LC-MS ES in the positive ion mode and by UV detection at 229 nm.

Name Code	Metabolite Peak	Compound Number	Ret. Time	Mol. Mass	Parent Ion
			min	*Da*	*m/z*
Demethylated 3-OH-nabumetone	M1		6.0	230	231 $[M + H]^+$
2,3-Diol nabumetone	M2, M3	6	8.5, 9.5	246	247 $[M + H]^+$
11.7 min metabolite	M4		11.7	ND	227
6-MNA	M5	9	13.2	216	239 $[M + Na]^+$
1-Hydroxy-nabumetone	M6	3	15.3	244	245 $[M + H]^+$
3-Hydroxy-nabumetone	M7	2	15.8	244	245 $[M + H]^+$
2-Hydroxy-nabumetone	M8	5	24.0	230	213 $[M + H - H_2O]^+$
Nabumetone	S	1	28.7	228	229 $[M + H]^+$

ND, not determined.

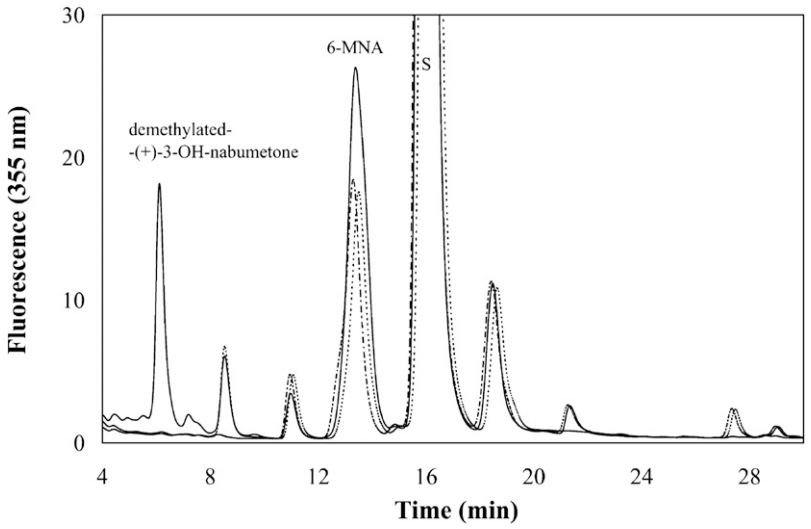

Fig. 2. RP-HPLC separation of the CYP1A2-catalyzed oxidation products of (+)-3-hydroxynabumetone [(+)-*R*-2]. The continuous line shows the regular enzymatic reaction, the dotted line shows the control reaction done in the absence of CPR/NADPH-generating system, and the dashed line shows the control done in the presence of the CYP1A2-inhibitor αNF. S stands for the (+)-3-hydroxynabumetone [(+)-*R*-2] substrate. The reactions were set up and analyzed as described in *Materials and Methods*.

1-hydroxynabumetone (3) (t_R = 15.3 minutes), albeit in lower yields (Fig. 1, Table 1). However, the CYP1A2-catalyzed oxidation of 1-hydroxynabumetone (3) yielded no more than trace amounts of 6-MNA (9) (Fig. 5). Interestingly, the 1-hydroxynabumetone (3) oxidation (Supplemental Fig. 3) revealed the presence of 3-(6-methoxynaphthalen-2-yl)propanoic acid (4) (t_R = 18.8 minutes), suggesting that CYP1A2 is able to also cleave the C1-C2 bond of 1. This metabolite was also observed in the oxidation of 1,2-diol (7), although ~10-fold less efficiently, most likely due to conversion of 1,2-diol (7) to 1-hydroxynabumetone (3) followed by C1-C2 cleavage. However, no 3-(6-methoxynaphthalen-2-yl)propanoic acid (4) was detected in the nabumetone (1) oxidation reaction, and furthermore this metabolite has not been reported in the literature.

CYP1A2-catalyzed oxidation of (+)-3-hydroxynabumetone (*R*-2), (−)-3-hydroxynabumetone (*S*-2), 1-hydroxynabumetone (3), 4-(6-methoxynaphthalen-2-yl)butan-2-ol (5), 4-(6-methoxynaphthalen-2-yl)butane-2,3-diol (6), 4-(6-methoxynaphthalen-2-yl)butane-1,2-diol (7), and 2-(6-methoxynaphthalen-2-yl)acetaldehyde (8) also produced their *O*-demethylated metabolites that eluted in the chromatogram between 4 and 7 minutes (Figs. 1–4). The *O*-demethylated metabolites of nabumetone, 6-MNA, 4-(6-methoxynaphthalen-2-yl)butan-2-ol, and 3-hydroxynabumetone were previously reported as either in vivo human metabolites of nabumetone (Haddock et al., 1984) or in vitro metabolites using liver microsomes or hepatocytes (Nobilis et al., 2013). However, this is the first demonstration that CYP1A2 catalyzes not only the 3-hydroxylation of nabumetone, but also *O*-demethylation of several nabumetone metabolites and dehydrogenation of a 2-hydroxyl moiety to the corresponding ketone.

P450 Enzymes Involved in Conversion of Nabumetone to 6-MNA

A previous study of the P450 isoform specificity of nabumetone oxidation surveyed a limited number of enzymes without examining the formation of reaction intermediates (Turpeinen et al., 2009). A broader panel of P450 enzymes was therefore tested for their possible involvement in nabumetone oxidation. This panel included (a) as purified proteins, CYP1A2, -2C8, -2C9, -2E1, -2J2, -2S1, -2W1, and -3A4; (b) as supersomes of cDNA expressed proteins, CYP1A1, -1A2, -1B1, -2B6, -2C18, -2C19, -2E1, and -3A4, all with coexpressed CPR; and finally (c) human liver microsomes and human intestinal microsomes (Fig. 6). Among the P450 enzymes tested are enzymes

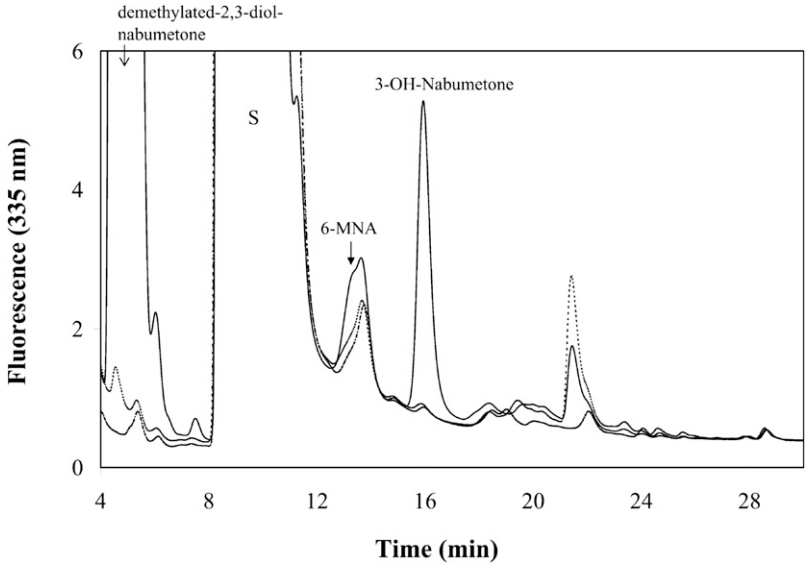

Fig. 3. RP-HPLC separation of the CYP1A2-catalyzed oxidation products of 2,3-diol-nabumetone (6). The continuous line shows the regular enzymatic reaction, the dotted line shows the control reaction done in the absence of CPR/NADPH-generating system, and the dashed line shows the control done in the presence of the CYP1A2-inhibitor αNF. S stands for the 2,3-diol-nabumetone (6) substrate. The reactions were set up and analyzed as described in *Materials and Methods*.

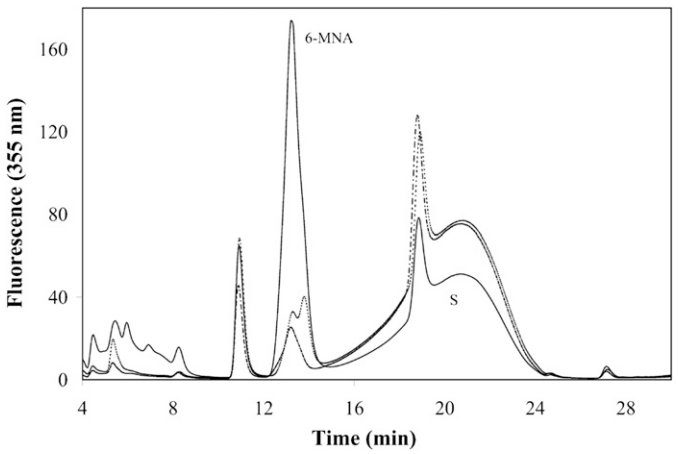

Fig. 4. RP-HPLC separation of the CYP1A2-catalyzed oxidation products of the aldehyde (8). The continuous line shows the regular enzymatic reaction, the dotted line shows the control reaction done in the absence of CPR/NADPH-generating system, and the dashed line shows the control done in the presence of the CYP1A2-inhibitor αNF. S stands for the aldehyde (8) substrate. The reactions were set up and analyzed as described in *Materials and Methods*.

that are highly expressed not only in the liver but also in extrahepatic tissues, including intestine, lung, or kidney. The oxidation of nabumetone by purified CYP2J2 and CYP3A4 was examined based on their reported involvement in nabumetone metabolism (Lee et al., 2010). Our results confirm that CYP1A2 is the enzyme that produces the greatest amount of 6-MNA, followed by CYP3A4 and CYP2B6 (Fig. 6). In contrast to the published results (Turpeinen et al., 2009), CYP2C19 and CYP2E1 did not reveal formation of 6-MNA, although they both show formation of significant amounts of 3-hydroxynabumetone (Fig. 6, inset). In contrast, CYP3A4 does generate 6-MNA and also shows formation of 3-hydroxynabumetone. The yield of 3-hydroxynabumetone among the P450 enzymes tested was the highest for CYP2C19, followed in descending order by CYP2B6, -3A4, -2E1, and -1A2 (Fig. 6, inset). CYP2J2 does oxidize nabumetone, but instead of forming 6-MNA produces 1-hydroxynabumetone (data not shown).

Nabumetone Oxidation by CYP1A2 Supported by Peroxides

Cytochrome P450 enzymes can oxidize many substrates via the peroxide shunt pathway in which the P450 catalytic cycle is supported by hydroperoxides rather than by molecular oxygen and the electron donor CPR. The CYP1A2-catalyzed oxidation of nabumetone by peroxides was therefore examined to determine in which steps of the reaction sequence molecular oxygen and CPR could be replaced by peroxides. In the event, nabumetone metabolites were obtained with cumene hydroperoxide (1 mM), but no products were detected with hydrogen peroxide (10 or 200 mM) or *tert*-butyl hydroperoxide (1 or 10 mM). Control reactions without either CYP1A2 or cumene hydroperoxide yielded no products. The time course of cumene-hydroperoxide-supported nabumetone oxidation revealed the greatest amount of products at longer incubations (30–60 minutes). The yield of products in a 60-minute incubation (Fig. 7) was up to 40-fold lower than that obtained in the normal enzymatic reaction (Fig. 1). The peroxide-dependent enzymatic oxidation yielded 3-hydroxynabumetone (2) (and the 11.7-minute metabolite), but no 6-MNA was detected. 6-MNA was not observed even when 3-hydroxynabumetone (2) was used as the substrate in the CYP1A2 shunt reaction, suggesting that 6-MNA formation is mediated by an iron-oxygen species distinct from that leading to the other nabumetone oxidation products. The identity of the metabolite eluted at 13.8 minutes (Fig. 7) was not determined; however, it is not 6-MNA and is also generated in the normal enzymatic reaction of nabumetone (Fig. 1).

As CYP3A4 also metabolizes nabumetone to 6-MNA, we examined the shunt reaction with this enzyme as well. Again, the results showed that 3-hydroxynabumetone (2) and the 11.7-minute metabolites were formed but not 6-MNA (data not shown). To determine whether peroxide-derived radicals could be involved in nabumetone oxidation under shunt pathway conditions, we performed the same reactions in the presence of free radical scavengers, either ascorbic acid (1 mM) or butylated hydroxytoluene (2 mM). The amounts of the products formed, including that of 3-hydroxynabumetone (2), were reduced up to twofold in the presence of the scavengers (data not shown), suggesting some role for free radicals in shunt-pathway nabumetone oxidation.

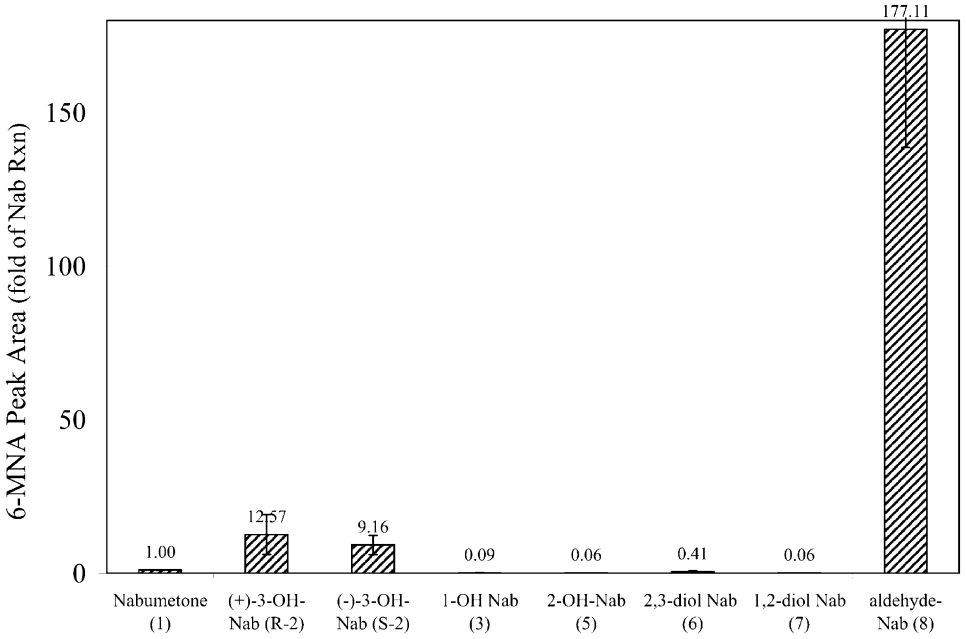

Fig. 5. Relative 6-MNA formation in the CYP1A2-catalyzed oxidation of nabumetone (1) and several possible intermediates (2–11). The data shown are the average of three independent experiments. The compound number is shown in parentheses after the compound name code. The numerical values are shown above each bar.

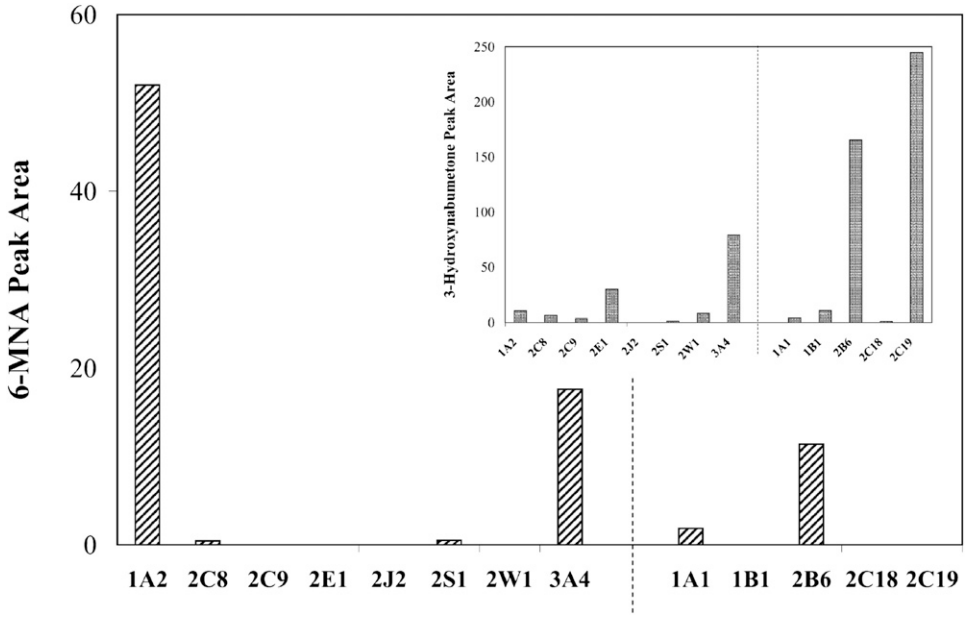

Fig. 6. 6-MNA formation in nabumetone oxidation by various P450 enzymes. 6-MNA formation, reported as the 6-MNA peak area, in nabumetone metabolism by (left) purified, reconstituted cytochrome P450 enzymes and (right) commercial supersomes. Inset: 3-Hydroxynabumetone formed in nabumetone oxidation reactions by P450 enzymes. The values shown are the average of two independent determinations.

In contrast, addition of ascorbic acid to the normal NADPH-dependent CYP1A2 reaction actually increased the efficiency of nabumetone metabolism and generated ~2-fold more 6-MNA (9) and 3-hydroxynabumetone (2) (Supplemental Fig. 4). This enhancement of the reaction by ascorbic acid, which establishes that ascorbic acid is not an inhibitor of the enzyme, may reflect protection of the enzyme from reactive oxygen species produced due to uncoupled turnover or some ability of ascorbic acid to donate electrons to the enzyme as a surrogate for CPR. CYP1A2 has been reported to be poorly coupled in the oxidation of phenacetin, for example (Yun et al., 2000).

The 11.7-Minute Metabolite

In addition to 6-MNA, the oxidation of nabumetone (1) by CYP1A2 generates a major peak for a metabolite with an HPLC retention time of 11.7 minutes when elution is monitored by absorbance at 229 nm or fluorescence at 355 nm. This metabolite is not observed in the absence of either CYP1A2 or the CPR/NADPH-generating system. Furthermore, it is not formed in significant amounts in CYP1A2-catalyzed oxidation of the nabumetone derivatives tested, (+)-3-hydroxynabumetone (2) (Fig. 2), 2,3-diol nabumetone (6) (Fig. 3), aldehyde-nabumetone (8) (Fig. 4), 1-hydroxynabumetone (3), 2-hydroxynabumetone (5), and 1,2-diol nabumetone (7), indicating that its formation is due to CYP1A2-catalyzed oxidation of nabumetone (1). Finally, this metabolite was also observed, albeit to a lesser extent, in the oxidation of nabumetone by CYP3A4, -2C9, and -2E1. LC-MS analysis of this metabolite gave a parent ion at *m/z* 227 (100%), which corresponds to a mass shift of −2 relative to nabumetone (*m/z* 229). Introduction of a C2-C3 double bond by either dehydrogenation or hydroxylation/dehydration could account for such a shift in mass. However, an authentic synthetic standard of the 2,3-desaturated derivative of nabumetone (11) had an HPLC retention time of 28 minutes, much later than the 11.7 minutes of the unknown metabolite. LC-MS analysis of the reaction employing $^{13}C,^{2}H_3$-methoxy labeled nabumetone gave an 11.7-minute metabolite with a molecular ion mass 4 units higher at *m/z* 231, demonstrating that the methoxy group was intact (Supplemental Fig. 5). Whatever modification has occurred must therefore be

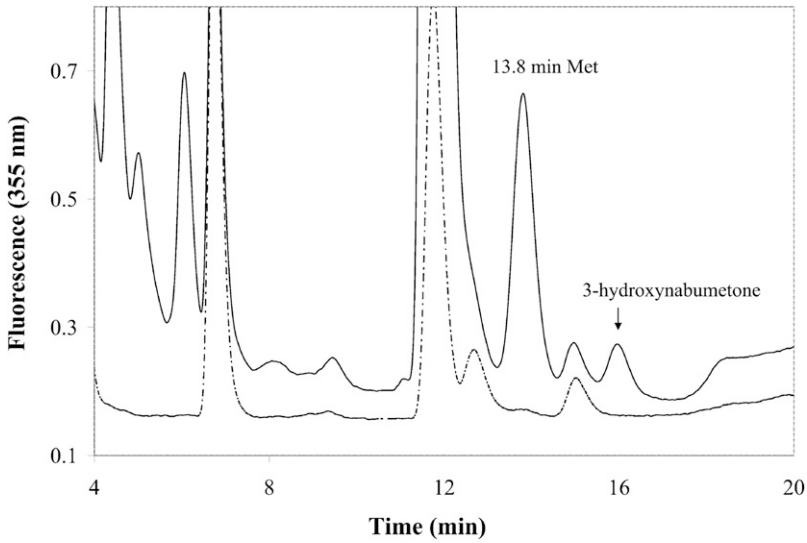

Fig. 7. RP-HPLC separation of the products formed in the cumene hydroperoxide-supported oxidation of nabumetone by CYP1A2. The continuous line shows the shunt reaction in the presence of CYP1A2, and the dashed line shows the control done in the absence of CYP1A2. CYP1A2 (0.5 μM) was incubated for 1 hour with nabumetone (0.2 mM) in the presence of DLPC (45 μM) and cumene hydroperoxide (1 mM).

localized to the naphthalene ring structure or the butyl side chain. We have not, however, definitively established the structure of this metabolite.

Discussion

Despite its long-term use in the clinic, the mechanism for conversion of the prodrug nabumetone to its active metabolite 6-MNA has remained unknown. To clarify this transformation, we synthesized a suite of potential intermediates and used them to identify the products formed in the metabolism of nabumetone by CYP1A2 and a range of other P450 enzymes. We also used them as substrates to further test whether they are precursors of 6-MNA and expanded the analysis of which human cytochrome P450 enzymes are involved in the conversion of nabumetone to its active metabolite. These studies establish unambiguously that the catalytic sequence involves CYP1A2-catalyzed 3-hydroxylation of nabumetone (1), carbon-carbon bond cleavage of 3-hydroxynabumetone (2) to the aldehyde 2-(6-methoxynaphthalen-2-yl)acetaldehyde (8), and finally oxidation of the aldehyde to the acid (9) (Scheme 2).

The specific role of CYP1A2 in the sequential oxidation of nabumetone to 3-hydroxynabumetone and 6-MNA was confirmed by the use of the purified, recombinant enzyme and by the demonstration that product formation did not occur in the absence of CPR/NADPH-generating system or in the presence of the CYP1A2 inhibitor αNF. 6-MNA was formed in higher yield in incubations of CYP1A2 with either (+)-3-hydroxynabumetone (*R*-2) or (−)-3-hydroxynabumetone (*S*-2) than with nabumetone and in much higher yield in incubations of the aldehyde 8, as expected for a sequence of transformation in which intermediates farther down the transformation pathway are used as substrates. Although the CY1A2 3-hydroxylation enantiospecificity was not examined, it is not relevant to the formation of 6-MNA, because both enantiomers were converted with a modest difference in efficiency to 6-MNA. The aldehyde 8 intermediate between 3-hydroxynabumetone and 6-MNA was not detected in CYP1A2-catalyzed nabumetone oxidation, but 8 is by far the best substrate of the three (Fig. 5) and is presumably not detected as an intermediate because it is converted so efficiently into 6-MNA. Interestingly, the nabumetone 3-hydroxylation reaction was catalyzed more effectively by CYP2C19, -2B6, and -3A4, but none of these three enzymes oxidized 3-hydroxynabumetone to 6-MNA nearly as efficiently as CYP1A2.

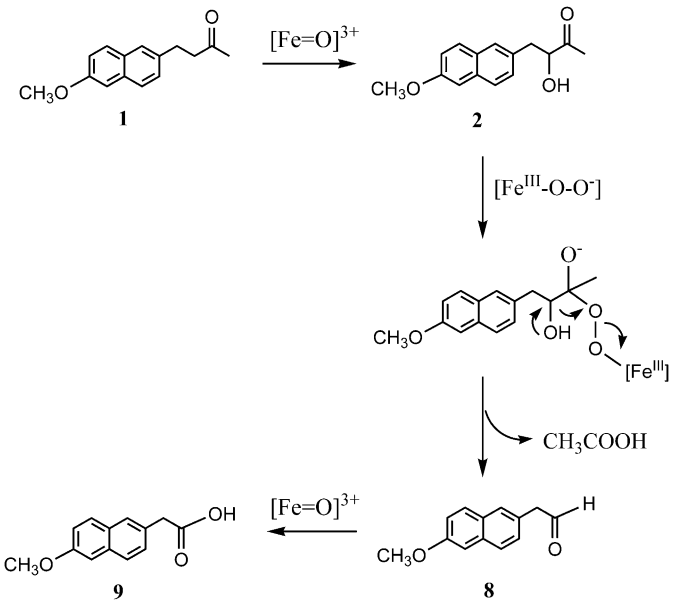

Scheme 2. Sequence of transformations in the P450-catalyzed oxidation of nabumetone to 6-MNA. The mechanism proposed for the carbon-carbon bond cleavage step is indicated. Numbers below structures indicate their compound number.

P450 enzymes that catalyze C-C bond cleavage reactions include CYP11 (cholesterol side chain cleavage), CYP19 (aromatase), CYP17 (sterol 17β-lyase), and CYP51 (lanosterol 14α-demethylase) (Ortiz de Montellano, 2005). Three types of substructures are represented by these reactions: (a) oxidation of a diol (CYP11), (b) oxidation of an isolated carbonyl group (CYP19, CYP51), and (c) oxidation of a carbonyl with an adjacent hydroxyl group (CYP17). A diol oxidation mechanism such as that catalyzed by CYP11 can be ruled out for nabumetone. Although the 2,3-diol (6) required can be generated in microsomal incubations by reduction of the 2-keto group followed by 3-hydroxylation or by reduction of the keto group in 3-hydroxynabumetone, it is a poor precursor of 6-MNA. The 6-MNA formed from conversion of 6 to 9 is readily explained by oxidation of the 2-hydroxyl (6) to the 2-keto (2) by CYP1A2, followed by normal conversion to 6-MNA (9). The observation that 3-hydroxynabumetone (2) is formed, that it is more efficiently converted to 6-MNA (9), and that no formation of 6-MNA is seen without 3-hydroxynabumetone formation disfavors a mechanism, such as that of CYP19 or CYP51, in which an isolated carbonyl group is oxidized. All the data, however, support a mechanism analogous to that of CYP17 in which the C-C bond scission involves oxidation of an α-hydroxy ketone.

Two mechanisms can be readily envisioned for C-C bond cleavage through P450 oxidation of an α-hydroxy ketone. In one of these, as postulated for CYP17 (Akhtar et al., 2011), the peroxy anion (Fe^{III}-O-O^{-}) intermediate in P450 catalysis adds to the carbonyl carbon as a nucleophile, producing a tetrahedral intermediate that subsequently fragments into a ketone and an acid (Scheme 2). The alternative mechanism involves hydrogen abstraction from the C3 alcohol group by the normal P450 ferryl species to give an oxygen radical that undergoes homolytic C-C bond scission. To distinguish between these two mechanisms, the CYP1A2 oxidation of nabumetone was carried out under shunt conditions that circumvent the ferric peroxy anion intermediate yet produce the final ferryl species. The finding that cumene hydroperoxide supported the formation of the hydroxylated products, including 3-hydroxynabumetone, but did not support the conversion of nabumetone or 3-hydroxynabumetone to 6-MNA, provides evidence that the oxidation proceeds via a CYP17-like mechanism involving ferric peroxy anion attack on the carbonyl group (Scheme 2). The fact that cumene hydroperoxide, but not hydrogen peroxide, supported the reaction raised the possibility that the cumyloxy radical might contribute to the observed oxidation. The oxidation reaction was modestly attenuated in the presence of the free radical scavengers ascorbic acid or butylated hydroxytoluene, but it is not clear if this is due to interception of cumene hydroperoxide-derived radical species or protection of the protein, because ascorbic acid promoted rather than inhibited the oxidation of nabumetone under normal CPR/NADPH-generating system conditions.

CYP1A2 exhibits multifunctional reactivity during nabumetone metabolism, performing not only hydroxylation and C-C cleavage but also *O*-demethylation and oxidation of the 2-hydroxyl group to a ketone in 4-(6-methoxynaphthalen-2-yl)butane-2,3-diol (6), 4-(6-methoxynaphthalen-2-yl)butane-1,2-diol (7) and 4-(6-methoxynaphthalen-2-yl)butan-2-ol (5). CYP1A2 can thus reverse the reduction of nabumetone recently shown to be performed by carbonyl-reducing enzymes in the liver (Skarydova et al., 2013). Of course, different binding orientations within the CYP1A2 active site are required for *O*-demethylation versus aliphatic chain hydroxylation and C-C bond cleavage.

Based on our results with purified CYP1A2, -2C8, -2C9, -2E1, -2J2, -2S1, -2W1 and -3A4 and supersomes of cDNA expressed CYP1A1, -1A2, -1B1, -2B6, -2C18, -2C19, -2E1, and -3A4, CYP1A2 is the major enzyme involved in the oxidation of nabumetone to 6-MNA. This conclusion agrees with that of Turpeinen et al. (2009), who tested supersomes of 11 cDNA expressed enzymes (CYP1A1, 1A2, 2A6, 2B6, 2C8, 2C9, 2C19, 2D6, 2E1, 3A4, 3A5). However, unlike their findings, CYP2E1 and -2C19 do not metabolize nabumetone to 6-MNA, whereas CYP3A4 yields 6-MNA, although threefold less than CYP1A2, and its binding affinity for nabumetone was also lower than that of CYP1A2. As the expression levels of CYP3A4 in human liver are severalfold higher than that of CYP1A2, CYP3A4 may play a significant role in nabumetone oxidation. Our results also establish that extrahepatic P450 enzymes such as CYP1A1, CYP1B1, and CYP2J2 do not play a significant role in oxidizing nabumetone to 6-MNA.

Acknowledgments

The authors thank Prof. Donghak Kim for making possible the year-long research work of Hyoung-Goo Park at UCSF. The authors also thank Santhosh Sivaramakrishnan for helpful discussions, Jonathan B. Johnston and David Maltby of the UCSF Mass Spectrometry facility for technical assistance, and the following individuals for generous gifts of purified proteins: Clinton Nishida for CYP2S1 and CYP2E1, Yan Zhao for CYP2W1, and YongQiang Wang for CYP3A4 and cytochrome b_5. Finally, the authors acknowledge a gift of commercial P450 enzymes and reagents from Elan Pharmaceuticals.

Authorship Contributions

Participated in research design: Varfaj, Zulkifli, De Voss, and Ortiz de Montellano.

Conducted experiments: Varfaj, Zulkifli, Park, and Challinor.

Contributed new reagents or analytic tools: Varfaj, Zulkifli, Park, and Challinor.

Performed data analysis: Varfaj, Zulkifli, Challinor, De Voss, and Ortiz de Montellano.

Wrote or contributed to the writing of the manuscript: Varfaj, Zulkifli, De Voss, and Ortiz de Montellano.

References

Akhtar M, Wright JN, and Lee-Robichaud P (2011) A review of mechanistic studies on aromatase (CYP19) and 17α-hydroxylase-17,20-lyase (CYP17). *J Steroid Biochem Mol Biol* **125**:2–12.

Berry EA and Trumpower BL (1987) Simultaneous determination of hemes a, b, and c from pyridine hemochrome spectra. *Anal Biochem* **161**:1–15.

Cho US, Park EY, Dong MS, Park BS, Kim K, and Kim KH (2003) Tight-binding inhibition by alpha-naphthoflavone of human cytochrome P450 1A2. *Biochim Biophys Acta* **1648**:195–202.

Dale JA and Mosher HS (1973) Nuclear magnetic resonance enantiomer regents. Configurational correlations via nuclear magnetic resonance chemical shifts of diastereomeric mandelate, O-methylmandelate, and alpha-methoxy-alpha-trifluoromethylphenylacetate (MTPA) esters. *J Am Chem Soc* **95**:512–519.

Goudie AC (1983) inventors, Beecham Group L, assignee. Naphthalene derivatives, a process for their preparation and their use in anti-inflammatory pharmaceutical compositions. U.S. patent 4382959 A. 10 May 1983.

Goudie AC, Gaster LM, Lake AW, Rose CJ, Freeman PC, Hughes BO, and Miller D (1978) 4-(6-Methoxy-2-naphthyl)butan-2-one and related analogues, a novel structural class of antiinflammatory compounds. *J Med Chem* **21**:1260–1264.

Guengerich FP, Martin MV, Sohl CD, and Cheng Q (2009) Measurement of cytochrome P450 and NADPH-cytochrome P450 reductase. *Nat Protoc* **4**:1245–1251.

Haddock RE, Jeffery DJ, Lloyd JA, and Thawley AR (1984) Metabolism of nabumetone (BRL 14777) by various species including man. *Xenobiotica* **14**:327–337.

Hedner T, Samulesson O, Wahrborg P, Wadenvik H, Ung KA, and Ekbom A (2004) Nabumetone: therapeutic use and safety profile in the management of osteoarthritis and rheumatoid arthritis. *Drugs* **64**:2315–2343; discussion 2344–2315.

Jacques J and Horeau A (1948) Structure moleculaire et activité oestrogene (VI). Preparation de quelques dérivés de l'acide amphihydroxynaphtyl β-propionique (acide allenolique). *Bull Soc Chim Fr* **15**:711–716.

Kelly DR (1999) A new method for the determination of the absolute stereochemistry of aromatic and heteroaromatic alkanols using Mosher's esters. *Tetrahedron Asymmetry* **10**:2927–2934.

Kim DH, Kim KH, Isin EM, Guengerich FP, Chae HZ, Ahn T, and Yun CH (2008) Heterologous expression and characterization of wild-type human cytochrome P450 1A2 without conventional N-terminal modification in *Escherichia coli*. *Protein Expr Purif* **57**:188–200.

Lee CA, Neul D, Clouser-Roche A, Dalvie D, Wester MR, Jiang Y, Jones JP, 3rd, Freiwald S, Zientek M, and Totah RA (2010) Identification of novel substrates for human cytochrome P450 2J2. *Drug Metab Dispos* **38**:347–356.

Mangan FR, Flack JD, and Jackson D (1987) Preclinical overview of nabumetone. Pharmacology, bioavailability, metabolism, and toxicology. *Am J Med* **83** (4B):6–10.

Matsumoto K, Nemoto E, Hasegawa T, Akimoto M, and Sugibayashi K (2011) In vitro characterization of the cytochrome P450 isoforms involved in the metabolism of 6-methoxy-2-napthylacetic acid, an active metabolite of the prodrug nabumetone. *Biol Pharm Bull* **34**: 734–739.

Messina A, Nencioni S, Gervasi PG, Gotlinger KH, Schwartzman ML, and Longo V (2010) Molecular cloning and enzymatic characterization of sheep CYP2J. *Xenobiotica* **40**:109–118.

Nishida CR, Lee M, and de Montellano PR (2010) Efficient hypoxic activation of the anticancer agent AQ4N by CYP2S1 and CYP2W1. *Mol Pharmacol* **78**:497–502.

Nobilis M, Mikušek J, Szotáková B, Jirásko R, Holčapek M, Chamseddin C, Jira T, Kučera R, Kuneš J, and Pour M (2013) Analytical power of LLE-HPLC-PDA-MS/MS in drug metabolism studies: identification of new nabumetone metabolites. *J Pharm Biomed Anal* **80**:164–172.

Ortiz de Montellano PR (2005) Cytochrome P450 Structure, Mechanism, and Biochemistry. KluwerAcademic/Plenum Publishers, New York

Pataki J, Di Raddo P, and Harvey RG (1989) An efficient synthesis of the highly tumorigenic anti-diol epoxide derivative of benzo[c]phenanthrene. *J Org Chem* **54**:840–844.

Patel BN, Sharma N, Sanyal M, Prasad A, and Shrivastav PS (2008) High-throughput LC-MS/MS assay for 6-methoxy-2-naphthylacetic acid, an active metabolite of nabumetone in human plasma and its application to bioequivalence study. *Biomed Chromatogr* **22**:1213–1224.

Porubsky PR, Meneely KM, and Scott EE (2008) Structures of human cytochrome P-450 2E1. Insights into the binding of inhibitors and both small molecular weight and fatty acid substrates. *J Biol Chem* **283**:33698–33707.

Schmidt JM, Tremblay GB, Plastina MA, Ma F, Bhal neé Basra S, Feher M, Dunn-Dufault R, and Redden PR (2005) In vitro evaluation of the anti-estrogenic activity of hydroxyl substituted diphenylnaphthyl alkene ligands for the estrogen receptor. *Bioorg Med Chem* **13**:1819–1828.

Singh R, Ting JG, Pan Y, Teh LK, Ismail R, and Ong CE (2008) Functional role of Ile264 in CYP2C8: mutations affect haem incorporation and catalytic activity. *Drug Metab Pharmacokinet* **23**:165–174.

Skarydova L, Nobilis M, and Wsól V (2013) Role of carbonyl reducing enzymes in the phase I biotransformation of the non-steroidal anti-inflammatory drug nabumetone in vitro. *Xenobiotica* **43**:346–354.

Turpeinen M, Hofmann U, Klein K, Mürdter T, Schwab M, and Zanger UM (2009) A predominate role of CYP1A2 for the metabolism of nabumetone to the active metabolite, 6-methoxy-2-naphthylacetic acid, in human liver microsomes. *Drug Metab Dispos* **37**: 1017–1024.

VanRheenen V, Kelly RC, and Cha DY (1976) Improved catalytic OsO_4 oxidation of olefins to *cis*-1,2-glycols using tertiary amine oxides as oxidant. *Tetrahedron Lett* **17**:1973–1976.

Varfaj F, Lampe JN, and Ortiz de Montellano PR (2012) Role of cysteine residues in heme binding to human heme oxygenase-2 elucidated by two-dimensional NMR spectroscopy. *J Biol Chem* **287**:35181–35191.

Viviano M, Glasnov TN, Reichart B, Tekautz G, and Kappe CO (2011) A scalable two-step continuous flow synthesis of nabumetone and related 4-aryl-2-butanones. *Org Process Res Dev* **15**:858–870.

Wang X, Medzihradszky KF, Maltby D, and Correia MA (2001) Phosphorylation of native and heme-modified CYP3A4 by protein kinase C: a mass spectrometric characterization of the phosphorylated peptides. *Biochemistry* **40**:11318–11326.

Wester MR, Yano JK, Schoch GA, Yang C, Griffin KJ, Stout CD, and Johnson EF (2004) The structure of human cytochrome P450 2C9 complexed with flurbiprofen at 2.0-A resolution. *J Biol Chem* **279**:35630–35637.

Wu ZL, Sohl CD, Shimada T, and Guengerich FP (2006) Recombinant enzymes overexpressed in bacteria show broad catalytic specificity of human cytochrome P450 2W1 and limited activity of human cytochrome P450 2S1. *Mol Pharmacol* **69**:2007–2014.

Yun CH, Miller GP, and Guengerich FP (2000) Rate-determining steps in phenacetin oxidations by human cytochrome P450 1A2 and selected mutants. *Biochemistry* **39**:11319–11329.

Address correspondence to: Paul R. Ortiz de Montellano, 600 16th St., N572D, San Francisco, CA 94158-2517. E-mail: Ortiz@cgl.ucsf.edu